Electronic Supplementary Material (ESI) for Materials Chemistry Frontiers.

Achieving Remarkable and Reversible Mechanochromism from Bright Ionic AIEgen with High Specificity for Mitochondria Imaging and Secondary Aggregation Emission Enhancement for Long-Term Tracking of Tumor

Xinzhe Yang,[+] Qian Wang,[+] Peiyu Hu, Chao Xu, Wenjing Guo, Zhi Wang, Zhu Mao, Zhan Yang, Cong Liu, Guang Shi,* Ling Chen,* Bingjia Xu,* Zhenguo Chi

Content

I. Experimental Section

Chemical Reagents and Materials.

4-(1,2,2-triphenylvinyl)benzaldehyde was prepared according to the literature method.[1] 2-(4-bromophenyl)acetonitrile, tetrakis(triphenylphosphine)palladium(0), pyridin-4-ylboronic acid, Aliquat 336, tetrabutylammonium hydroxide (40 wt.% solution in MeOH), iodomethane and potassium hexafluorophosphate were purchased from Innochem or *J&K* Scientific Ltd and used as received. All other reagents and solvents were purchased from Zeyuan Company (Guangzhou, China) with analytical grade and used without further purification.

Measurements

Nuclear magnetic resonance (^{1}H NMR and ^{13}C NMR) was carried out on a Bruker AVANCE 400 MHz spectrometer by using DMSO-d_6 as solvent and tetramethylsilane as internal standard. Mass spectra were conducted on the instrument of LTQ_Orbitrap_LCMS (LTQ Orbitrap Elite). Powder XRD patterns were recorded by an X-ray diffractometer (Rigaku, Ultima IV) in a scanning rate of 4° (2θ)/min at 293 K. Thermal behaviors for the samples of TCPy and TCPyP were determined by differential scanning calorimetry (DSC) at a heating rate of 10 ^{o}C/min under nitrogen atmosphere using a TA Q20 thermal analyzer. Photoluminescent spectra were recorded on an Ocean Optics spectrophotometer (QE65 Pro). UV-vis absorption spectra were achieved on a Hitachi UV-3900H or SHIMADZU UV-3600 spectrophotometer. Absolute PL quantum yields (PLQYs) and lifetimes of the samples were measured by using an Edinburgh FLS980 spectrometer which is equipped with a calibrated integrating sphere. Data of single-crystal X-ray diffraction was collected from an Agilent Technologies Gemini A Ultra system with Cu-K_α radiation (λ = 1.54178 Å) at 150 K and was solved by using Olex2 program suite to give single crystal structures of the compounds. CCDC numbers for this article are 1948629 and 1948630. Photoluminescent images demonstrating the mechanochromic phenomena were taken by a Canon T5i digital camera with a Canon 50 mm f/1.8G STM camera lens.

Theoretical calculations

Theoretical calculation based on DFT at the 6–311G** level was conducted on a Gaussian 16 program. The molecular geometries of TCPy and TCPyP were directly selected from their single crystal structures and were submitted for the simulations of Kohn-Sham frontier orbitals without further optimization. Intermolecular interaction analyses for the molecules in single crystal structures were carried out by Multiwfn with independent gradient model (IGM).[2-4]

TPA Measurements

The TPA spectra of TCPy and TCPyP in water/DMSO (95:5 v/v) were measured by TPIF spectroscopy using Rhodamine B in methanol as standard (concentration: 10 μM).[5] The samples were excited by a Ti:Sapphire laser (Spectra-Physics ® Inspire TM ultrafast OPO) with central wavelength of 800 nm, pulse duration of 100 fs and repetition rate of 82 MHz. In the measurement system, monochrometer (IsoPlane 160) and CCD (PIXIS400) from Princeton instrument were

used for signal collection. TPA cross-sections of these two samples were calculated by the following equation:

$\delta_2 = \delta_1(F_2 n_2^2 \Phi_1 C_1)/(F_1 n_1^2 \Phi_2 C_2)$

where the subscripts 1 and 2 stand for the standard and sample molecules; F is the two-photon fluorescence intensity; Φ is the fluorescence quantum yield; C is the molar concentration and n is the refractive index of the solvent.[6] The TPA cross-section (δ) of Rhodamine B at 800 nm is 120 GM.[7]

Cell Culture

A549 cell line was maintained in a medium (Dulbecco's Modified Eagle Medium (DMEM basix 1×), Gibco) that contains 10% fetal bovine serum (FBS，Gibco) at 37 ℃ under a water-saturated atmosphere with 5% CO_2 (Series II water jacket CO_2 incubator, Thermo Fisher Scentific).

Cytotoxicity by CCK8 Assay

Cytotoxicities of TCPy and TCPyP were studied by the method of Cell Counting Kit-8 (CCK8, DOJINDO). The nanosuspensions of TCPy and TCPyP were diluted to different concentrations by using DMEM complete medium. The resulting mixtures of the emitters were inoculated onto precultured A549 cell monolayers (~5×10^4) in 96-well plates and were incubated at 37 ℃ for 4 h, respectively. After washing with DPBS for three times, the CCK8 medium mixture (100 μL/well) was added to the plates and incubated at 37 ℃ for 1.5 h. Afterwards, the absorbance values of the samples at 450 nm were measured with a microplate reader (BioTek EPOCH2 microplate reader, BioTek insruments Inc).

Two-photon imaging

A549 cells were precultured on a 35 mm glass bottom dish (Nunc) with a bottom diameter of 27 mm. The cells were incubated with TCPy or TCPyP (5 μM) for 2 h and mitotracker green (Thermo Fisher, 200 nM) for 45 min. Before imaging, they were washed with DPBS for three times. Two-photon imaging was then implemented on confocal microscope (710 NLO, Zeiss), and intense fluorescent signals were observed in the cytoplasm of the live cells.

In vivo imaging

All experimental procedures involving animals were performed according to the institutional ethical guidelines for animal experiments at the Guangzhou Institute of Biomedicine and Health, Chinese Academy of Sciences. The tumor models were implanted (5×10^5 A549 cells in 100 uL DPBS) subcutaneously in each posterior flank of the 5- to 6-week-old athymic nude mice bought from Beijing Vital River Laboratory Animal Technology Co. Ltd. Animals were followed for tumor growth about 1 months (the volume of the tumor about 1.5 cm×0.5 cm), and TCPyP (10 mM, 100 μL) was subsequently injected into one of the two tumors or the vein of mouse. Concurrently, the other tumor of the mouse was selected as negative control. Live images of the mouse were obtained at different time by IVIS Spectrum (IVIS 200, Xenogene).

Hematoxylin and eosin (H&E) staining

The inject section were fixed in 4% polyoxymethylene overnight, washed with PBS and dehydrated in 70% ethanol before paraffin embedding. The sections were cut into 4–5 μm, and mounted on glass slides after the tissue were fixed and embedded in paraffin. The slide stained in Mayer's hematoxylin solution and 1% eosin Y solution for hematoxylin and eosin staining.

Synthesis

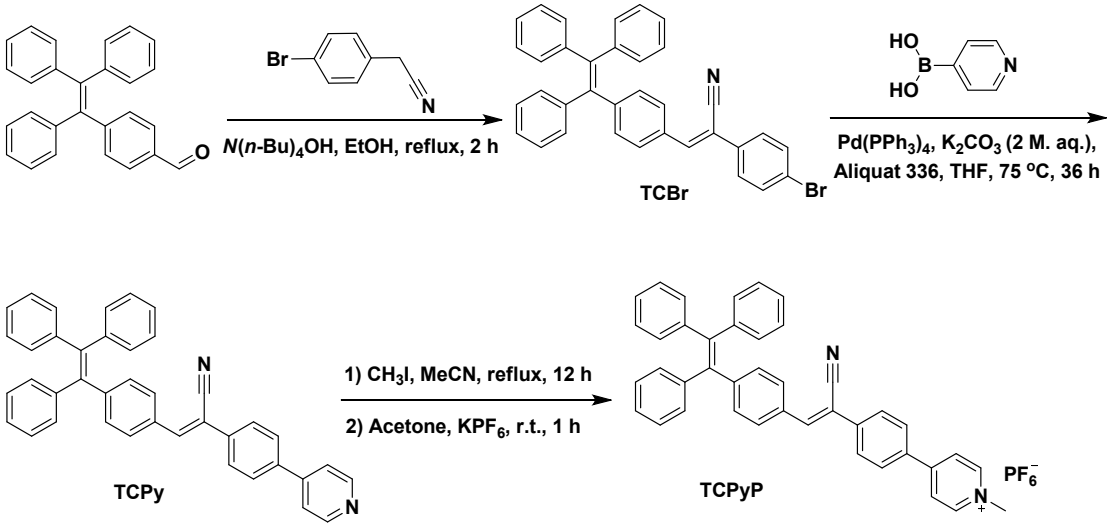

Scheme S1. Synthetic routes of the target compounds.

General procedures for synthesis of the emitters

Synthesis of compound TCBr 4-(1,2,2-Triphenylethenyl)benzaldehyde (1.00 g, 2.76 mmol), 4-bromophenylacetonitrile (0.54 g, 2.77 mmol), ethanol (40 mL) and tetrabutylammonium hydroxide (8 drops) were sequentially added into a 250 mL three-necked flask. The mixture was heated to reflux and stirred under argon for 2 h. After cooling to room temperature, the precipitate was filtered and washed with ethanol for three times to give a bluish green power. Yield: 75% (1.12 g). ^{1}H NMR (400 MHz, DMSO-d_6) δ 8.00 – 7.94 (s, 1H), 7.88 – 7.62 (m, 6.4 Hz, 6H), 7.22 – 7.09 (m, 11H), 7.07 – 6.95 (dd, J = 15.9, 7.6 Hz, 6H). ^{13}C NMR (101 MHz, DMSO-d_6) δ 146.39, 143.25, 143.05, 142.22, 140.12, 133.59, 132.48, 131.95, 131.68, 131.13, 131.08, 131.01, 129.21, 128.42, 128.39, 128.24, 128.12, 127.32, 127.20, 127.17, 122.88, 118.06, 108.85. ESI-MS m/z: $[M]^+$ calcd. for, 537.1092; found, 537.1080.

Synthesis of TCPy A flask was charged with **TCBr** (1.00 g, 1.86 mmol), pyridin-4-yl-4-boronic acid (0.29 g, 2.32 mmol), potassium carbonate (0.64 g, 4.64 mmol, 2 M aqueous solution), $Pd(PPh_3)_4$ (50 mg, 0.04 mmol) and THF (40 mL). The mixture was then degassed and stirred at 75 °C under argon for 36 h. After cooling to room temperature, the reaction mixture was concentrated, and the resulting crude product was purified by silica gel column chromatography with DCM/ethanol (v/v=50:1) as eluent. TCPy was further recrystallized from

dichloromethane/methanol to give a light green powder in 36% yield. (0.36 g). ^{1}H NMR (400 MHz, DMSO-d_6) δ 8.73 – 8.56 (d, J = 4.9 Hz, 2H), 8.04 – 7.98 (s, 1H), 7.96 – 7.81 (dd, J = 34.9, 8.4 Hz, 4H), 7.79 – 7.66 (m, 4H), 7.24 – 7.04 (m, 11H), 7.03 – 6.90 (dd, J = 17.1, 8.0 Hz, 6H). ^{13}C NMR (101 MHz, DMSO-d_6) δ 150.20, 145.87, 145.70, 142.73, 142.69, 142.55, 141.71, 139.62, 137.49, 134.56, 131.53, 131.16, 130.61, 130.57, 130.48, 128.75, 127.92, 127.88, 127.74, 127.45, 126.82, 126.70, 126.66, 126.36, 121.00, 117.71, 108.73. ESI-MS m/z: $[M+H]^+$ calcd. for, 537.2330; found, 537.2321.

Synthesis of TCPyP Compound **TCPy** (0.20 g, 0.37 mmol), iodomethane (0.20 mL) and acetonitrile (30 mL) were added into a 250 mL three-necked flask. The mixture was heated to reflux and stirred for 12 h. After cooling to room temperature, the reaction mixture was poured into diethyl ether, and an orange precipitate was obtained. Subsequently, the resulting solid powder, acetone and saturated KPF6 solution (10 mL) were added to a three-necked flask. The mixture was stirred at room temperature for 1 h. The precipitates were then filtered and washed with water for several times to give a yellow solid powder in 77% yield (0.20 g). ^{1}H NMR (400 MHz, DMSO-d_6) δ 9.13 – 8.95 (d, J = 6.6 Hz, 2H), 8.64 – 8.50 (d, J = 6.6 Hz, 2H), 8.28 – 8.18 (d, J = 8.4 Hz, 2H), 8.17 – 8.12 (s, 1H), 8.03 – 7.94 (d, J = 8.4 Hz, 2H), 7.84 – 7.74 (d, J = 8.3 Hz, 2H), 7.23 – 7.10 (m, 11H), 7.06 – 6.97 (d, J = 17.6, 8.3 Hz, 6H), 4.39 – 4.29 (s, 3H). ^{13}C NMR (101 MHz, DMSO-d_6) δ 152.93, 146.27, 145.56, 143.99, 142.72, 142.70, 142.51, 141.85, 139.59, 137.14, 133.64, 131.36, 131.24, 130.61, 130.59, 130.49, 128.96, 128.73, 127.93, 127.90, 127.75, 126.84, 126.73, 126.65, 123.93, 117.54, 108.23, 47.01. ESI-MS m/z: $[M\text{-}PF_6^-]^+$ calcd. for, 551.2482; found, 551.2470.

II. Photophysical Properties of the MC-Active AIEgens from Literatures

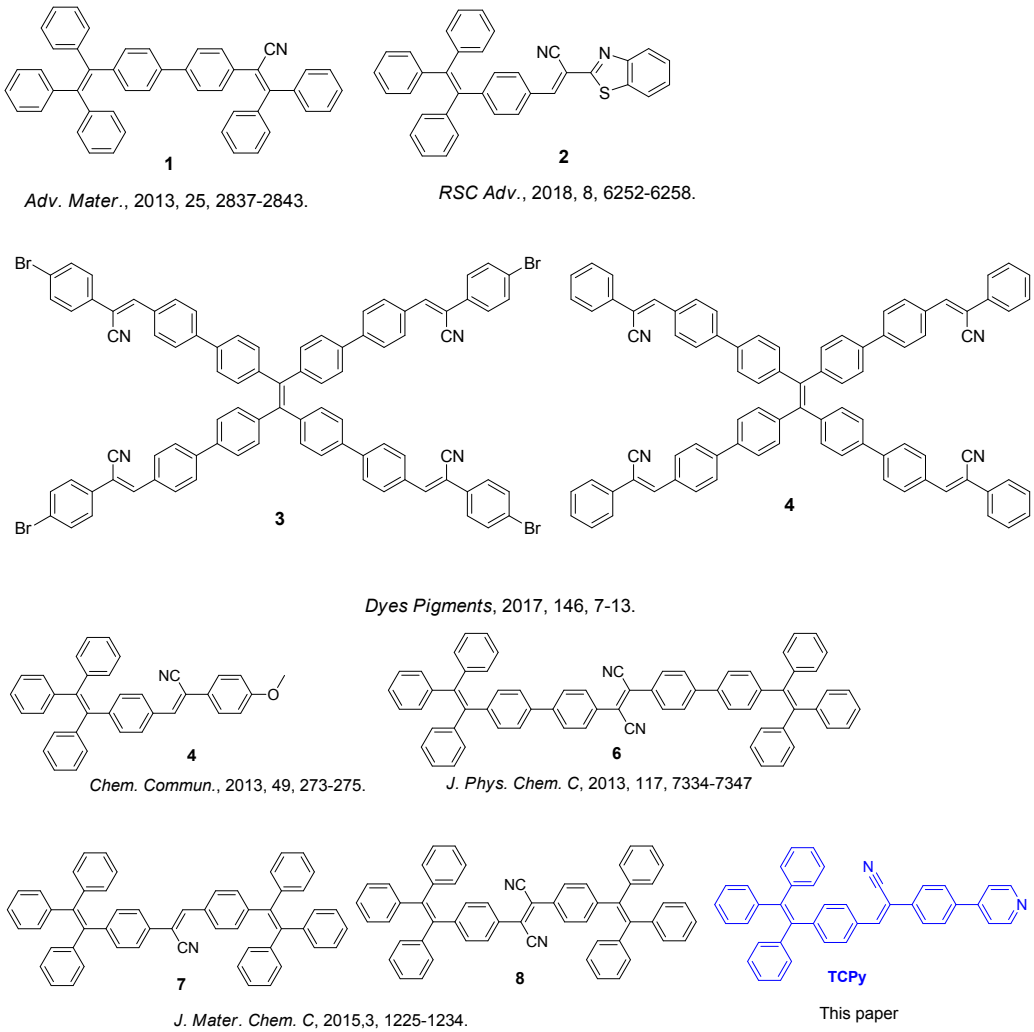

Fig. S1 Molecular structures of the representative organic compounds with moieties of tetraphenylethene and phenylacrylonitrile.

Table S1. Mechanochromic properties of the representative organic compounds with moieties of tetraphenylethene and phenylacrylonitrile

Compound	$\lambda_{em,pristine}$ (nm)	$\Phi_{pristine}$ (%)	$\lambda_{em,ground}$ (nm)	Φ_{ground} (%)	$\Delta\lambda_{em}$ (nm)	Reversibility Performance
1	443	52.5	515	42.0	72	Excellent
2	497	50.0	567	40.0	70	Poor
3	527	64.3 [a]	556	–	29	–
4	525	72.7 [a]	552	–	27	Excellent
5	469	85.0	513	66.0	44	Excellent
TCPy	512	90.0	526	62.0	14	Excellent
6	541	100 [b]	563	–	22	Excellent
7	491	–	515	–	24	Excellent
8	517	–	567	–	50	Excellent

[a] In THF/water mixture with 80% water fraction; the quantum yield was measured by using 9,10-diphenylanthracene as standard. [b] In solid thin film.

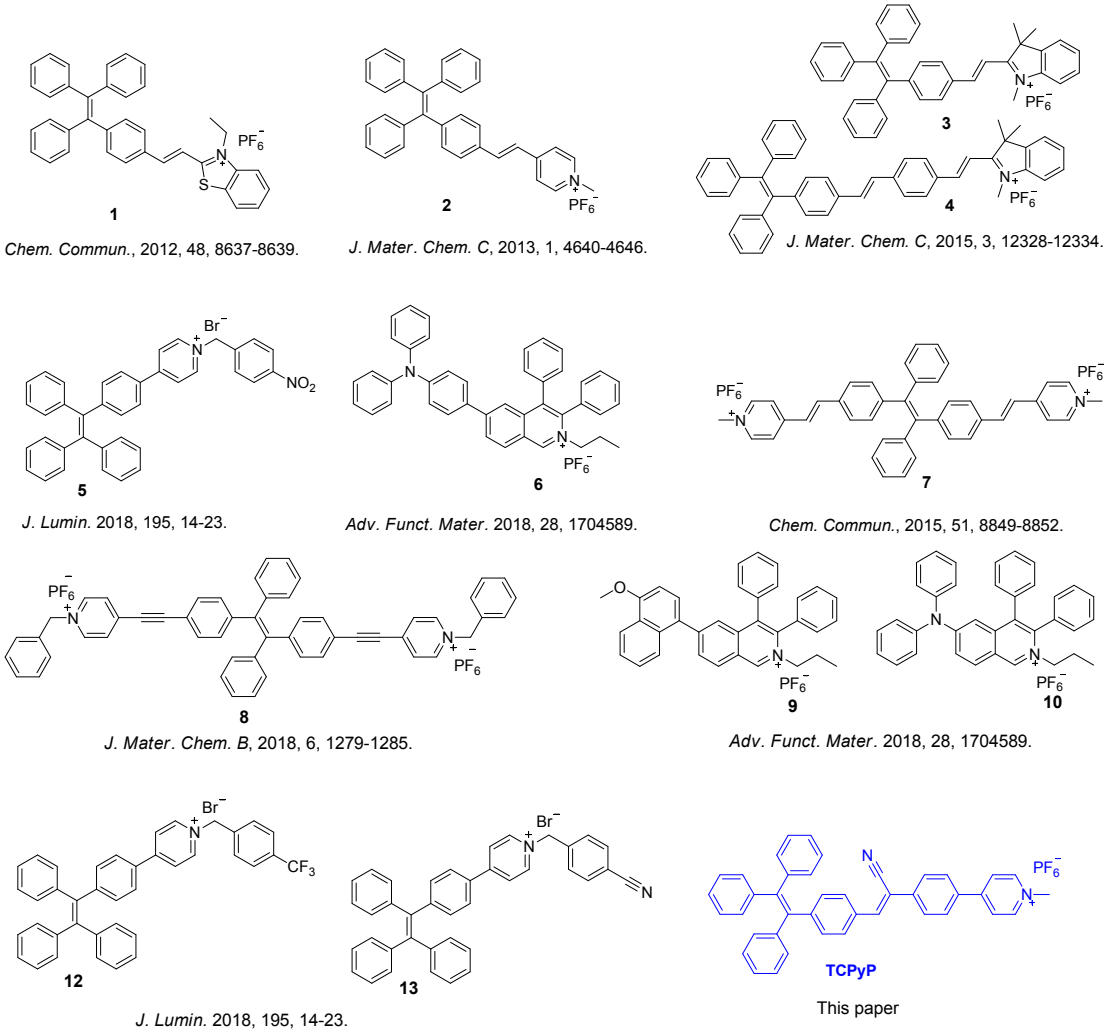

Fig. S2 Molecular structures of the reported organic salts with AIE and MC properties.

Table S2. Photophysical properties of the reported organic salts with AIE and MC characteristics.

Compound	$\lambda_{em,pristine}$ (nm)	$\Phi_{pristine}$ (%)	$\lambda_{em,ground}$ (nm)	Φ_{ground} (%)	$\Delta\lambda_{em}$ (nm)	Reversibility Performance
1	565	18.0	650	–	85	Excellent
2	515	31.8	600	20.4	85	Excellent
3	603	11.19	678	15.27	75	Excellent
4	638	10.19	707	3.71	69	Excellent
5	510	1.70	571	–	61	Excellent
6	563	19	623	–	60	–
7	560	43.0	605	18.0	45	Excellent
8	533	43.7	576	–	43	Poor
9	496	53	547	–	51	Poor
10	520	57	559	–	39	–
11	530	36.30	567	–	37	Excellent
12	510	4.60	559	–	49	Excellent
TCPyP	527	52	617	33	90	Excellent

III. Photophysical and Morphological Properties of TCPy and TCPyP

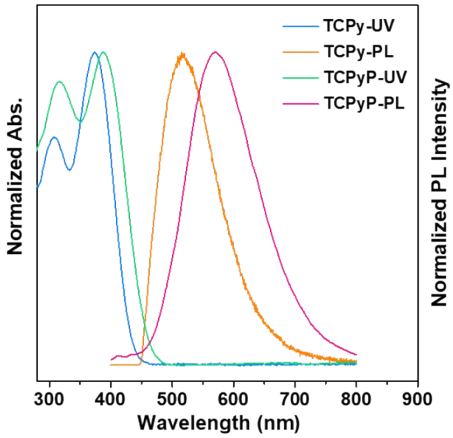

Fig. S3 UV-visible absorption and PL spectra of the compounds in 1,4-dioxane. (Concentration: 10 μM)

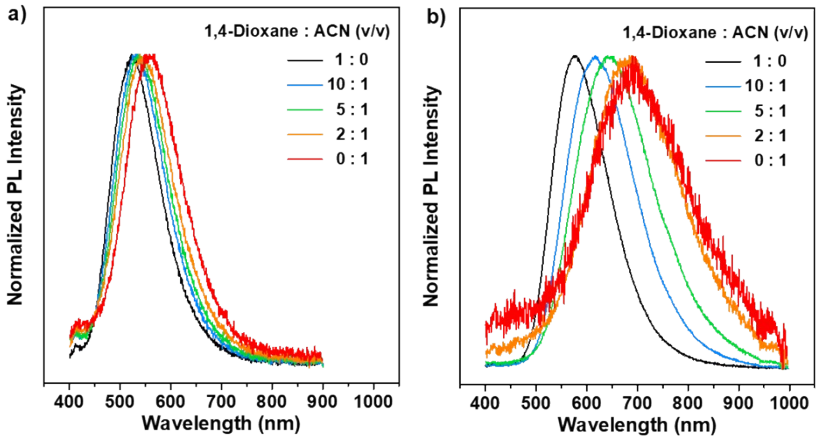

Fig. S4 PL spectra of TCPy a) and TCPyP b) in mixtures of 1,4-dioxane and acetonitrile with different volume ratios. (Concentration: 10 μM)

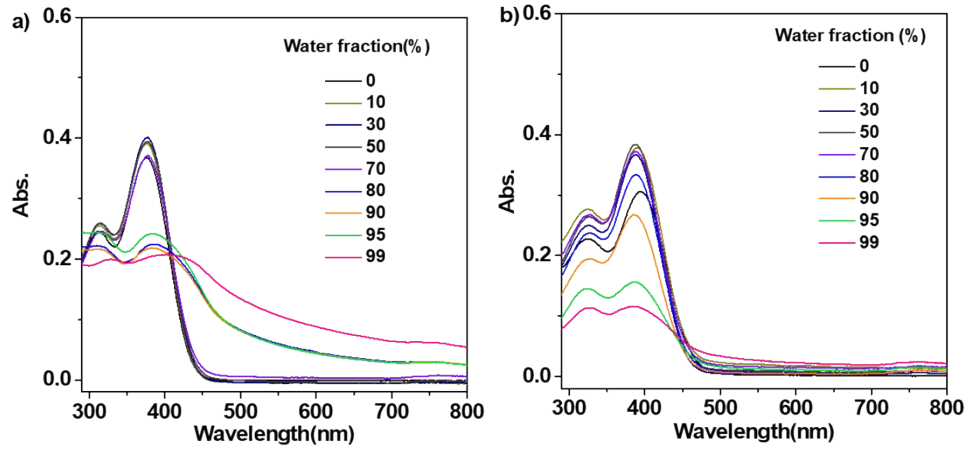

Fig. S5 UV-visible absorption spectra of TCPy a) and TCPyP b) in water/THF mixtures with different water fractions. (Concentration: 10 μM).

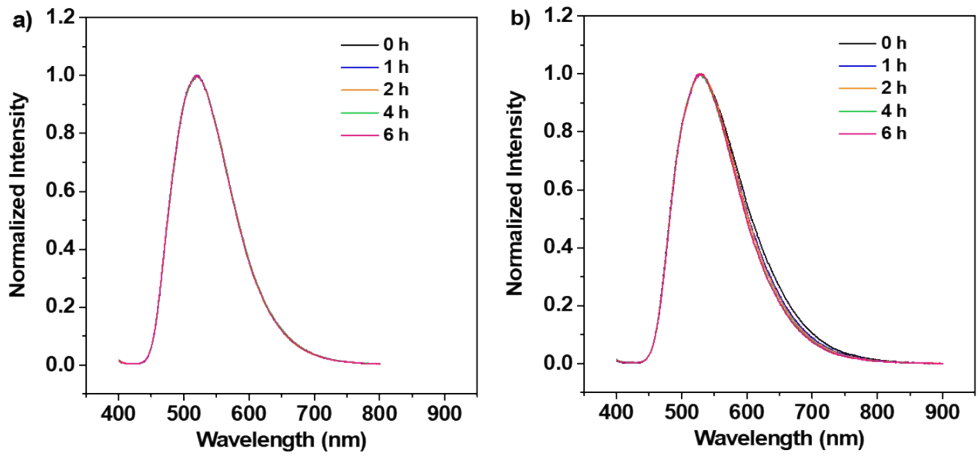

Fig. S6 PL spectra of the nanoaggregates of TCPy a) and TCPyP b) in the mixtures of water/THF with 99% water fraction at different standing time. (Excitation: 365 nm; Concentration: 10 μM)

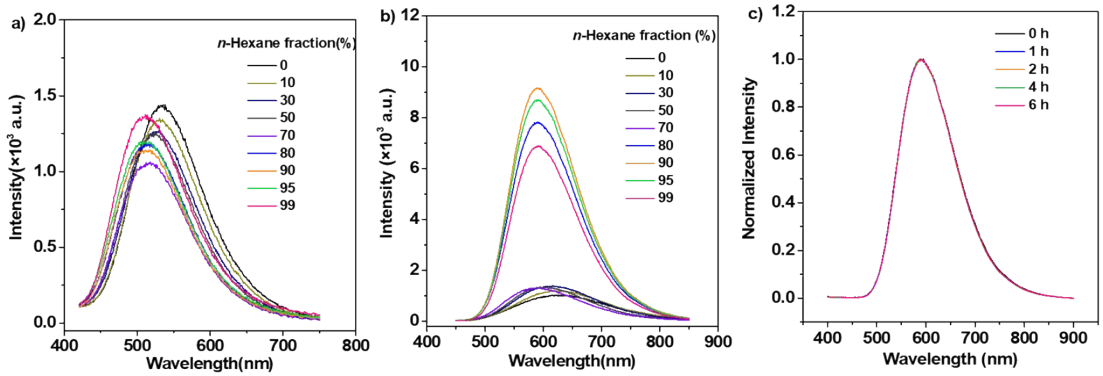

Fig. S7 PL spectra of the dilute solutions of TCPy a) and TCPyP b) in *n*-hexane/THF mixtures with different *n*-hexane fractions. c) PL spectra of the nanoaggregates of TCPyP in *n*-hexane/THF with 90% *n*-hexane fraction at different standing time. (Excitation: 365 nm; Concentration: 10 μM). By prolonging the standing time, the emission of TCPyP in the mixture of *n*-hexane/THF

with 90% *n*-hexane fraction was unchanged, suggesting that the molecular packing mode of TCPyP nanoaggregates is stable in the mixture.

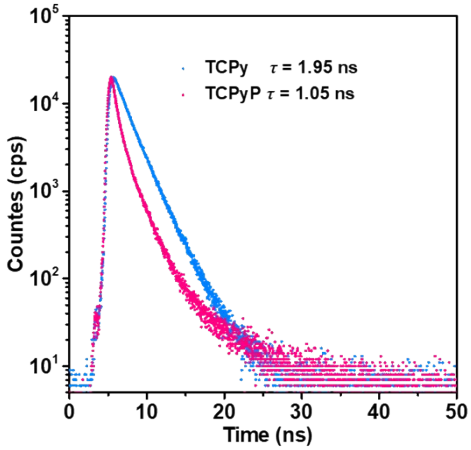

Fig. S8 Emission decay curves of the pristine samples of TCPy and TCPyP.

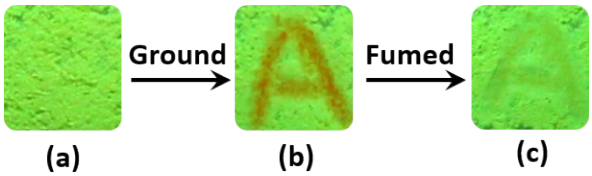

Fig. S9 Fluorescent images of TCPyP thin film on a filter paper without (a) and with (b) letter "A" being written by using a metal spatula. The image in (c) was obtained by fuming the film in dichloromethane vapour for about 10 min.

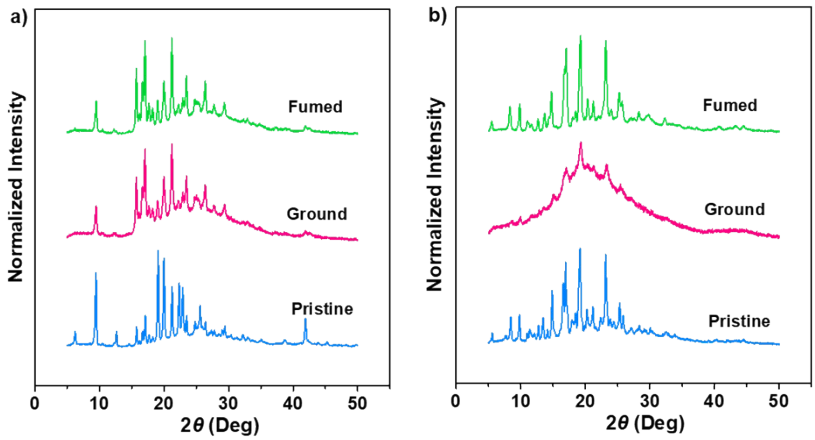

Fig. S10 Changes of XRD patterns for the samples of TCPy a) and TCPyP b) upon grinding.

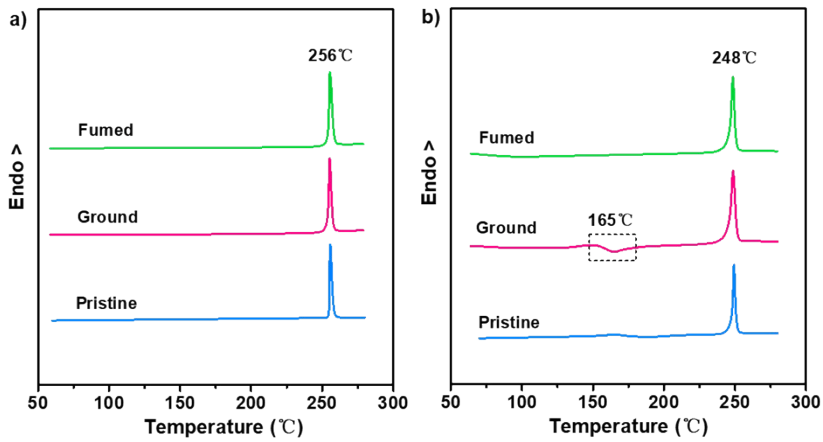

Fig. S11 DSC curves for the samples of TCPy a) and TCPyP b) upon grinding.

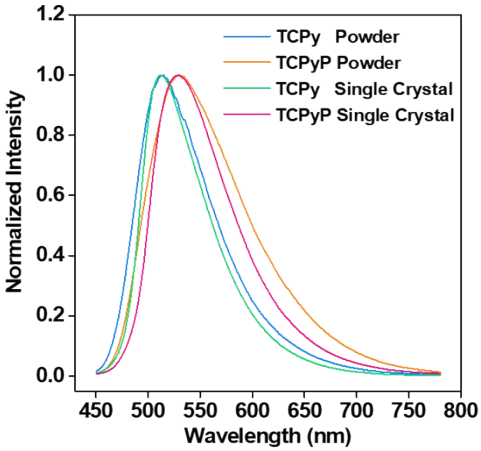

Fig. S12 PL spectra of solid powders and single crystals of TCPy and TCPyP.

IV. Mechanism Study for the Mechanochromism of TCPy and TCPyP

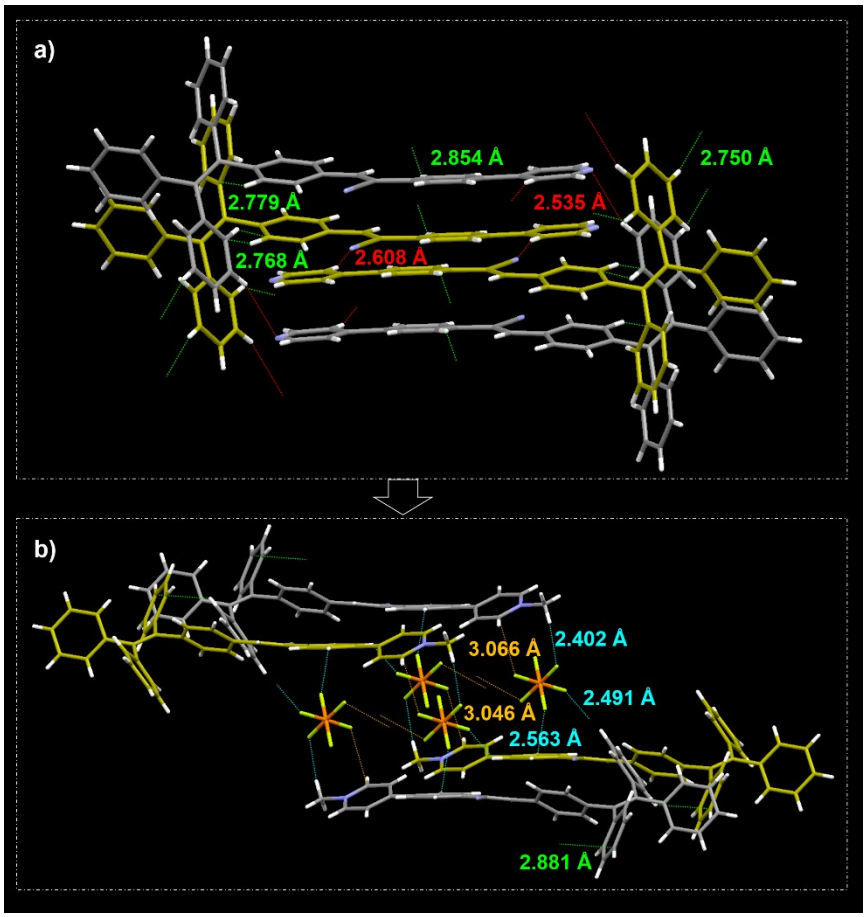

Fig. S13 Molecular packings and intermolecular interactions of TCPy a) and TCPyP b) in single crystal structures.

As depicted in Figure S13, two types of C-H···N interactions (with distances of 2.608 and 2.535 Å) and four types of C-H···π interactions (with distances of 2.750, 2.768, 2.779 and 2.854 Å) were observed in the single crystal structure of TCPy. These intense multiple interactions help to solidify the molecular conformations and stabilize the crystal structure. However, in the case of TCPyP, hexafluorophosphate anions inserted into the interstices among the molecules and enlarged the intermolecular distance from 3.033 Å to 5.314 Å (distance between the planes of two pyridine rings). The C–H···N hydrogen bonds and most of C–H···π interactions were thus replaced by C-H···F (three types with distances of 2.402, 2.491 and 2.536 Å) and P-F···C (two types with distances of 3.046 and 3.066 Å) interactions which were all built by the hexafluorophosphate anions and the methylated phenylpyridine fragments. That is, the insertion of hexafluorophosphate slightly weakened the intermolecular interactions, offering opportunity for the generation of high contrast MC via intermolecular slippage.

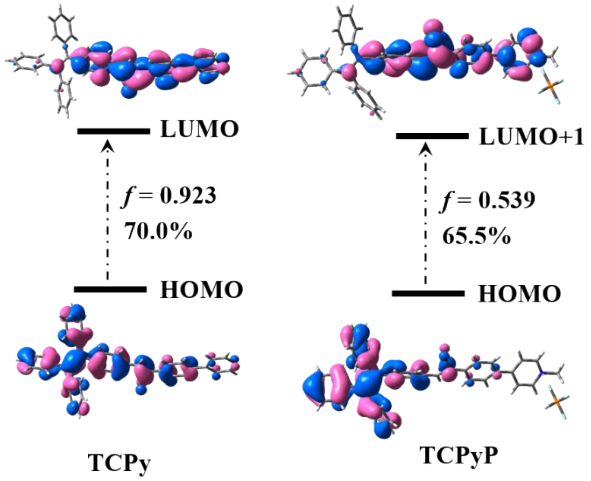

Fig. S14 Kohn-Sham frontier orbitals for the molecules of TCPy and TCPyP in single crystal structures.

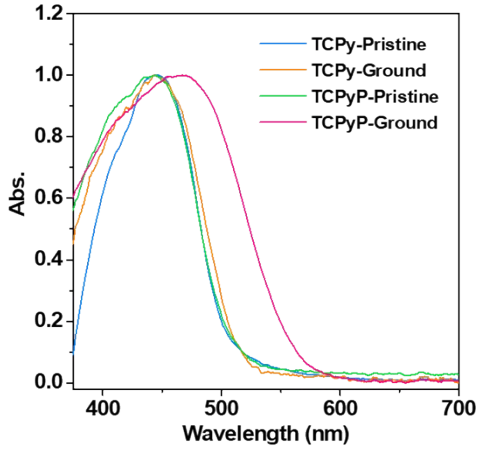

Fig. S15 UV-visible absorption spectra for the pristine and ground samples of TCPy and TCPyP

V. In Vitro and In Vivo Bioimaging

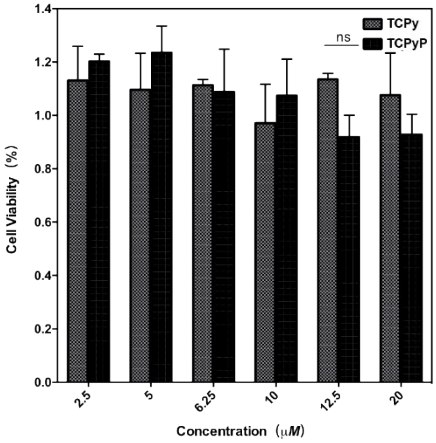

Fig. S16 Cytotoxicities of different treatments with a series of doses of TCPy and TCPyP against A549 cancer cells for 4 hours by CCK8 assay.

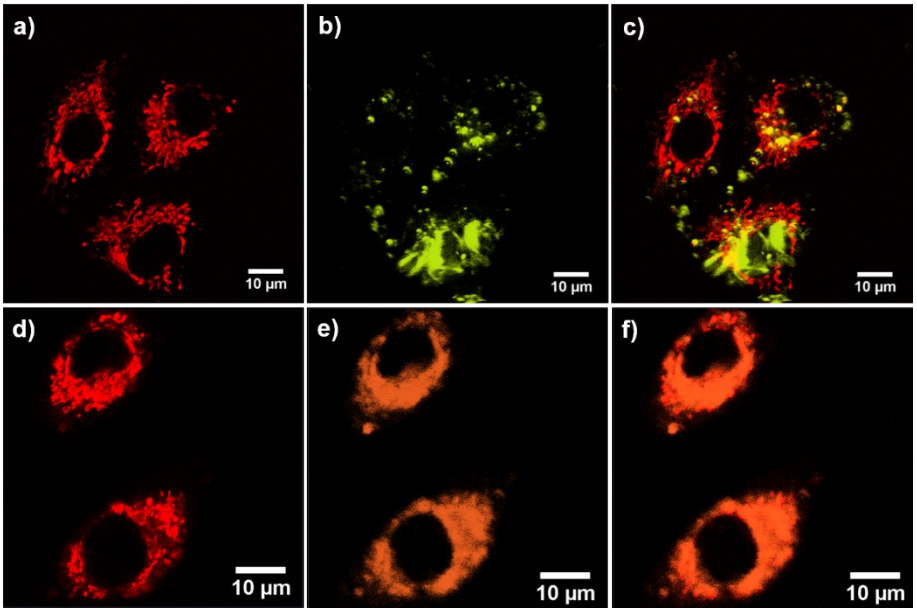

Fig. S17 CLSM images indicate the colocalization of MitoTracker Deep Red FM with TCPy a–c) and TCPyP d–f) in A549 cancer cells, respectively. a,d) Fluorescent image of mitochondria stained by MitoTracker Deep Red FM (red pseudocolor). b) Two-photon excited fluorescent image of mitochondria stained by TCPy. c) An overlay image of parts a) and b). e) Two-photon excited fluorescent image of mitochondria stained by TCPyP. f) An overlay image of parts d) and e). (Excitation: 800 nm; Concentration: 5 μM)

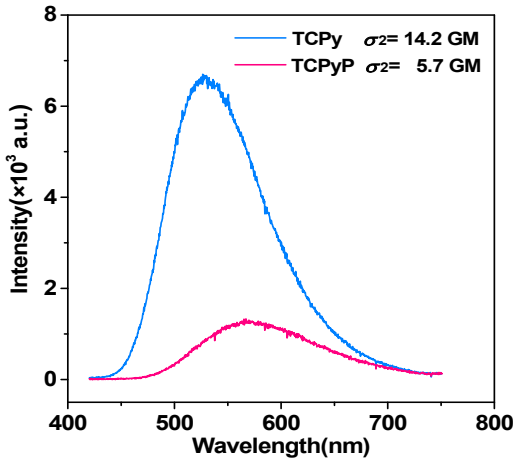

Figure S18. Two-photon excited fluorescence spectra and two photon-absorption cross-sections of TCPy and TCPyP at 800 nm in DMSO/H_2O mixtures with 95% water fractions.

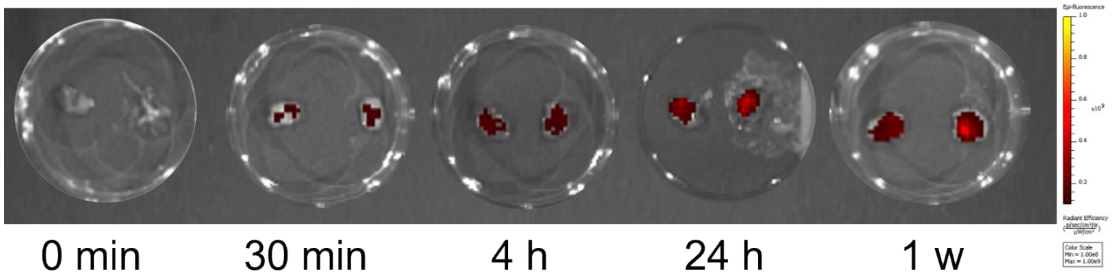

Fig. S19 *In vivo* imaging by intravenous injection: *ex vivo* fluorescent imaging of the tumors at different time from the mice injected with TCPyP.

VI. ^{1}H NMR, ^{13}C NMR and Mass Spectra and Single Crystal Structural Information of the Compounds

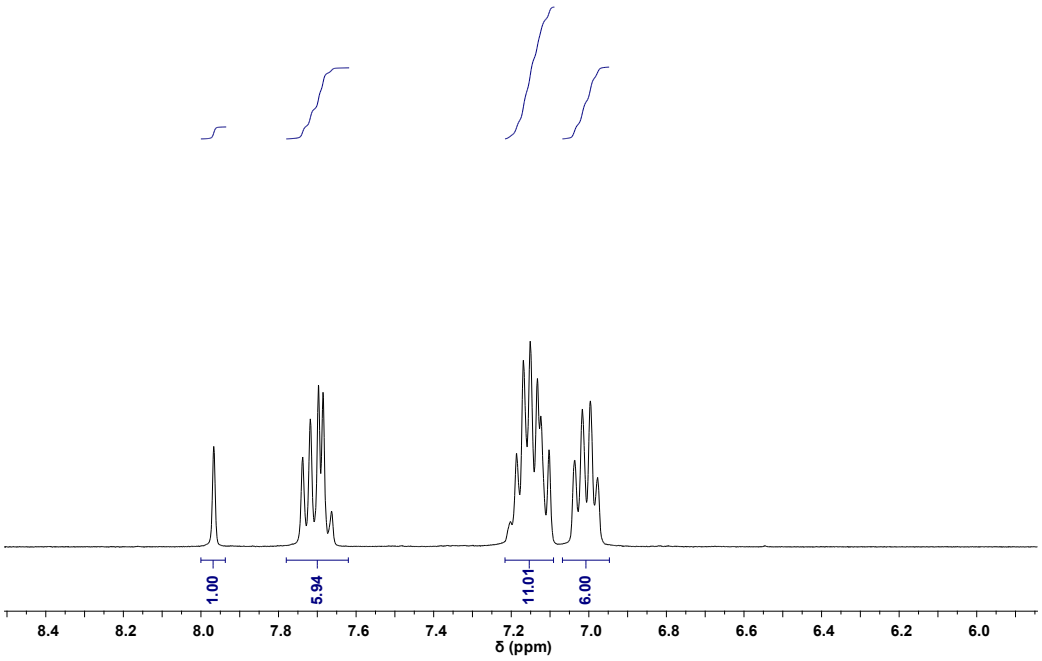

Fig. S20 ^{1}H NMR spectrum of TCBr (in DMSO-d_6).

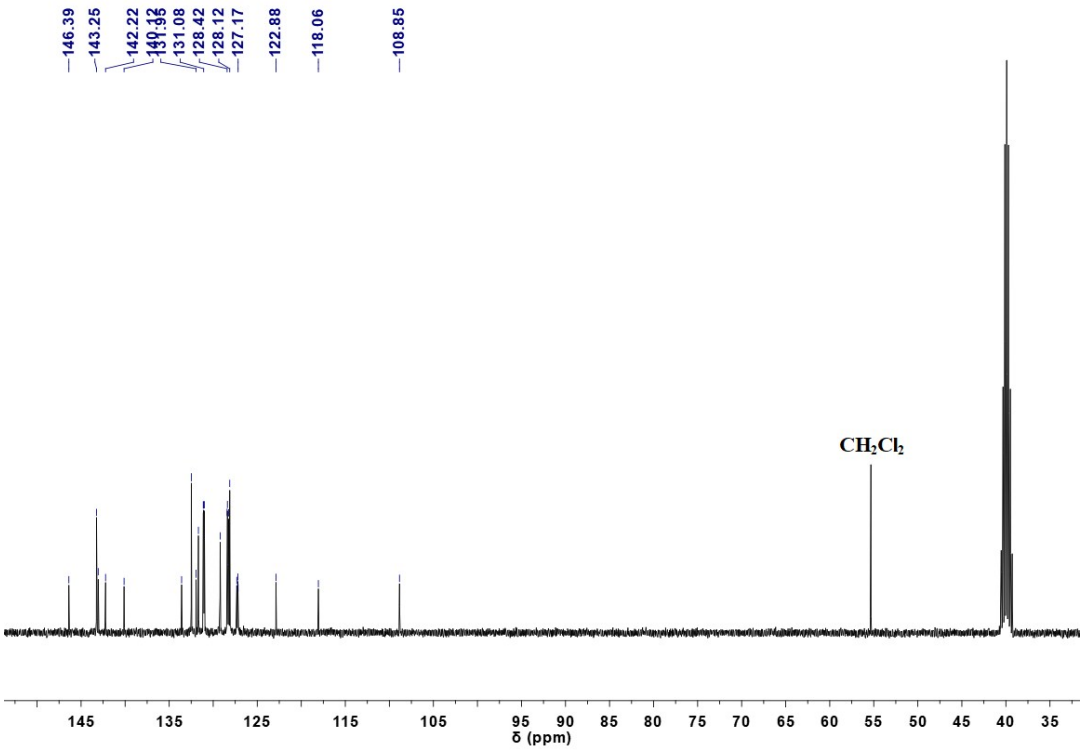

Fig. S21 ^{13}C NMR spectrum of TCBr (in DMSO-d_6).

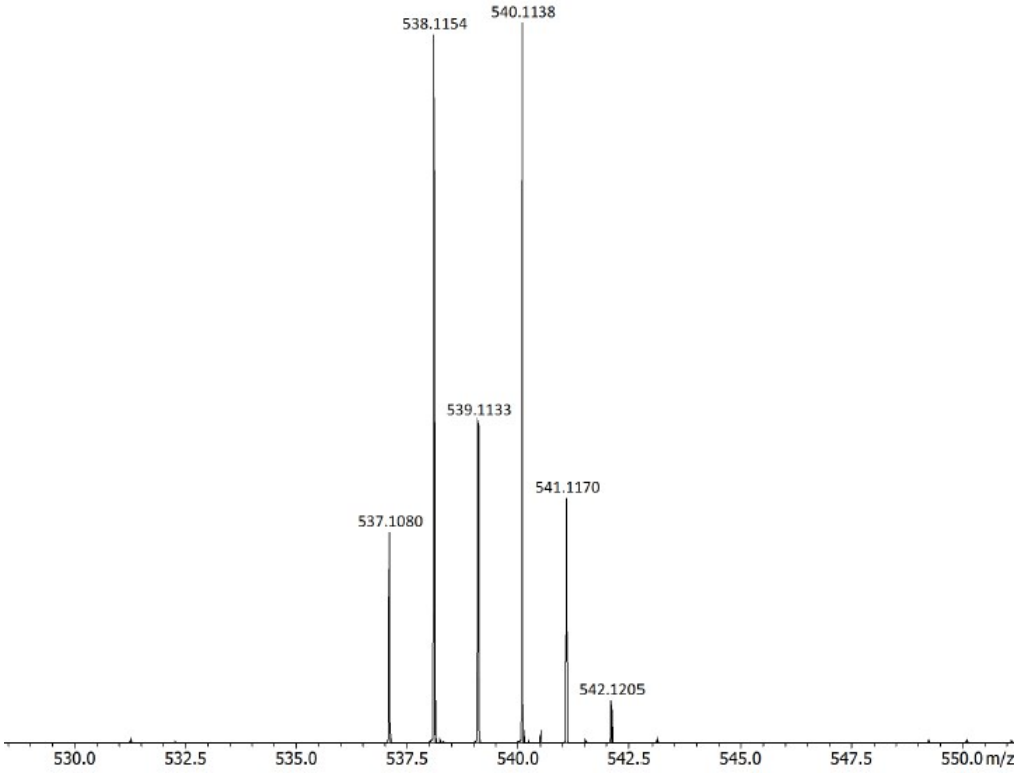

Fig. S22 ESI-MS of TCBr.

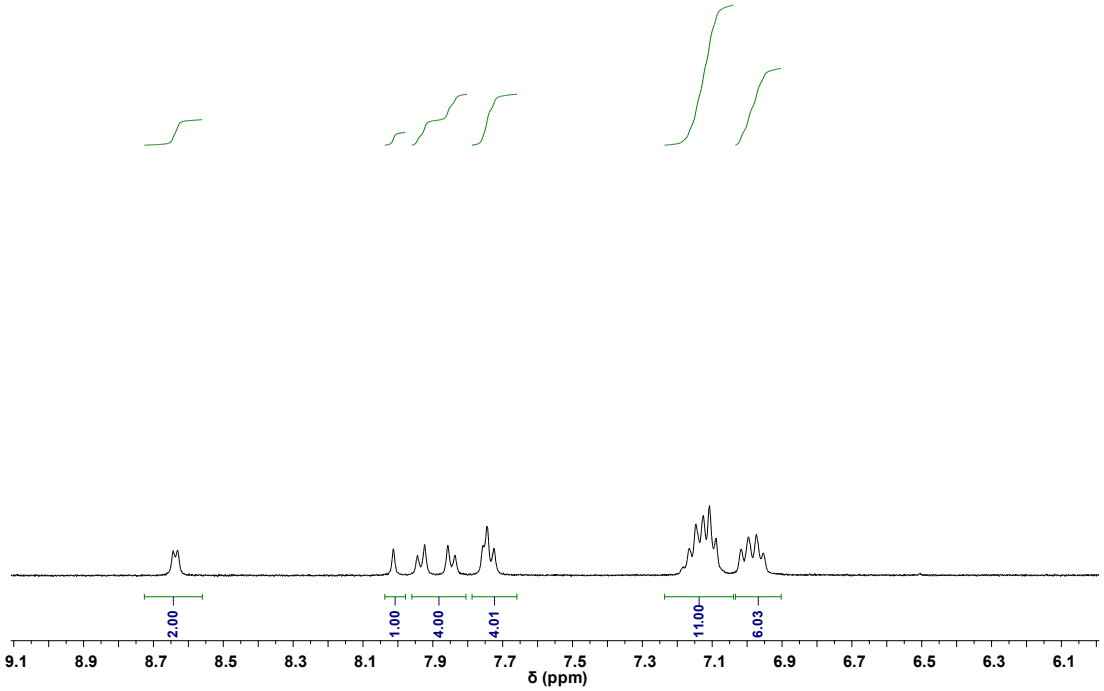

Fig. S23 ^{1}H NMR spectrum of TCPy (in DMSO-d_6).

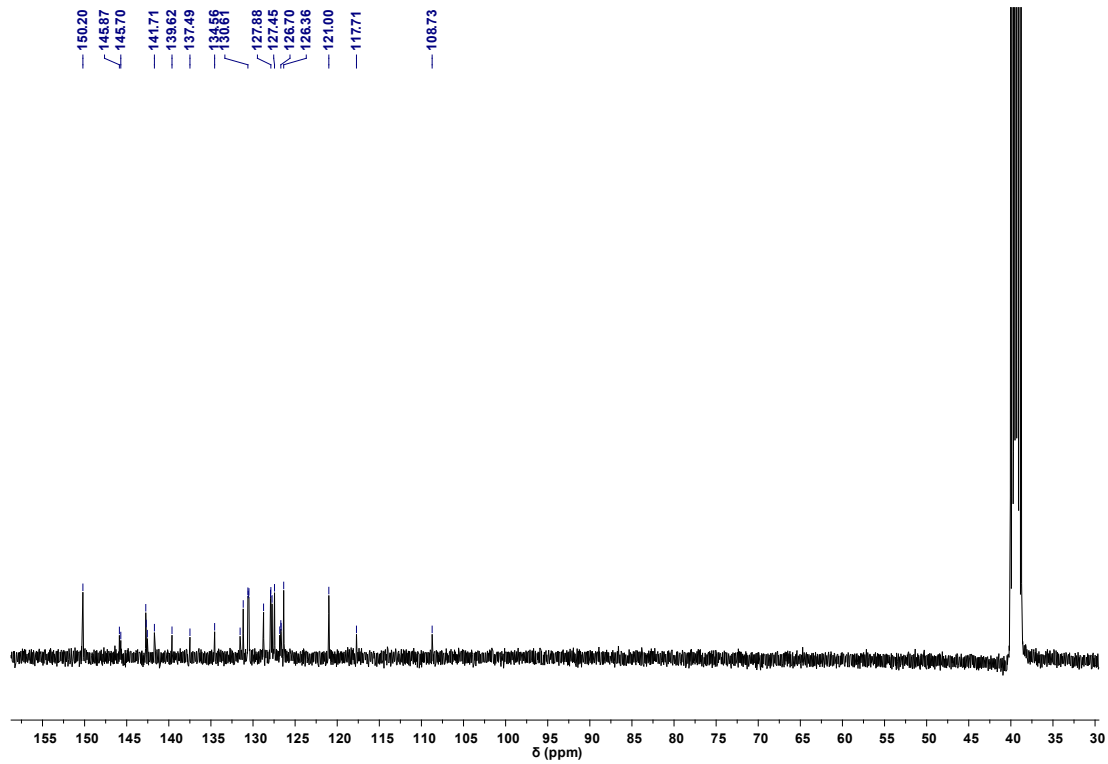

Fig. S24 ^{13}C NMR spectrum of TCPy (in DMSO-d_6).

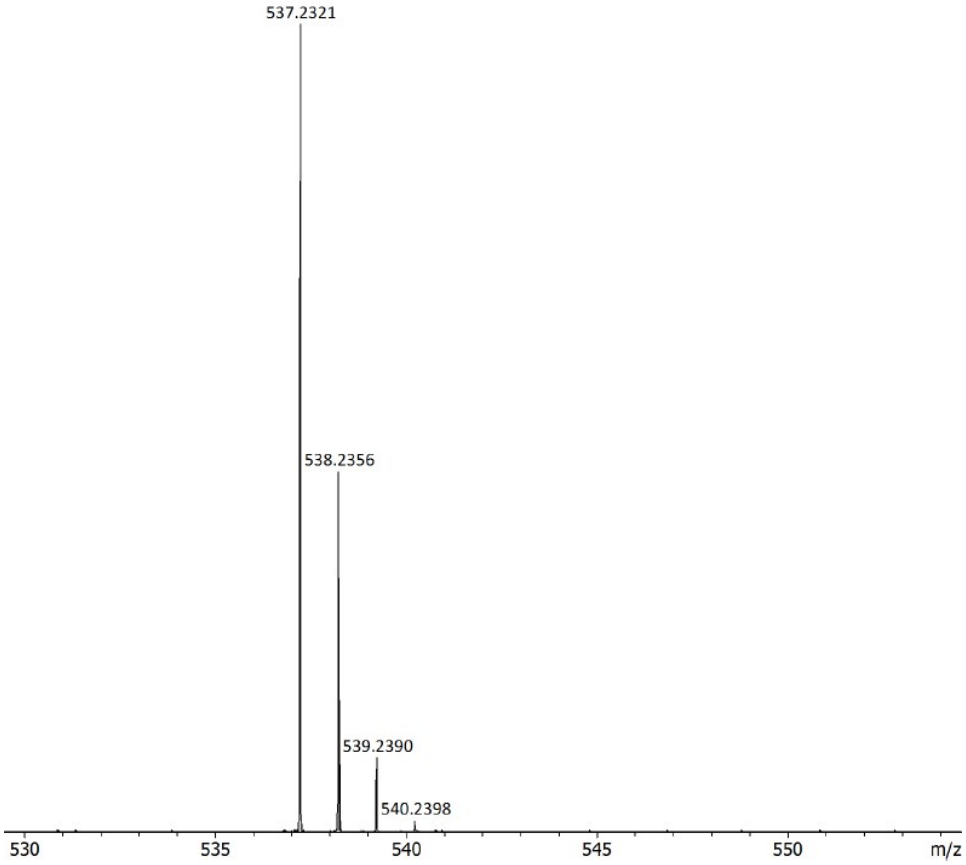

Fig. S25 ESI-MS of TCPy.

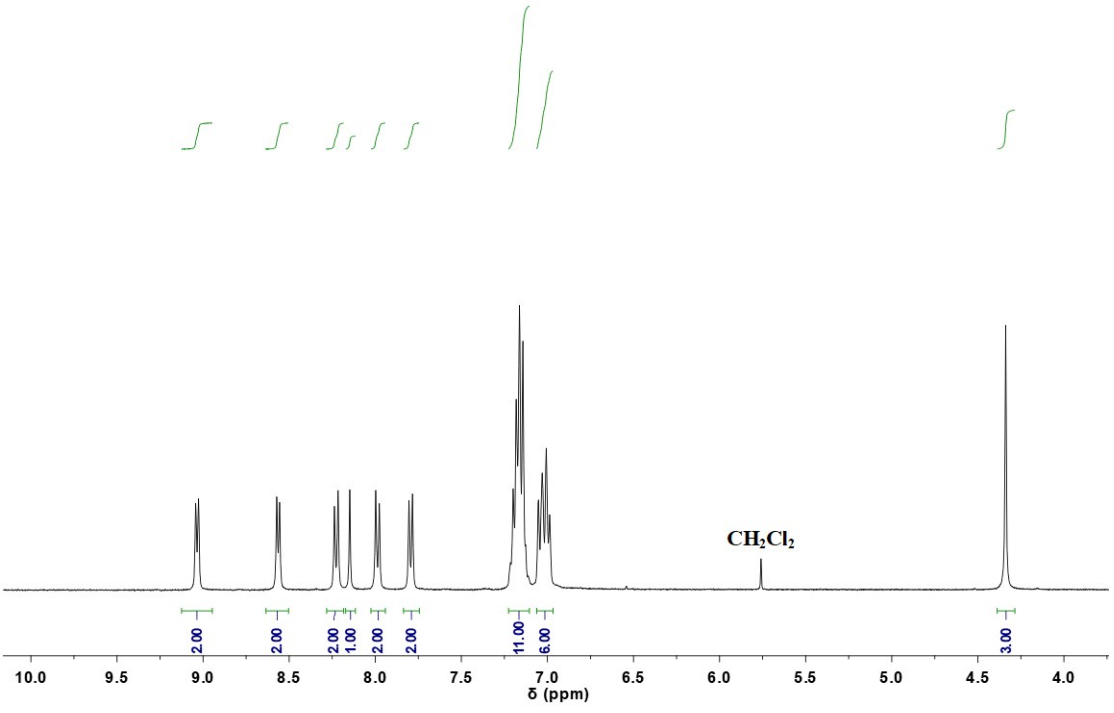

Fig. S26 ^{1}H NMR spectrum of TCPyP **(**in DMSO-d_6**)**.

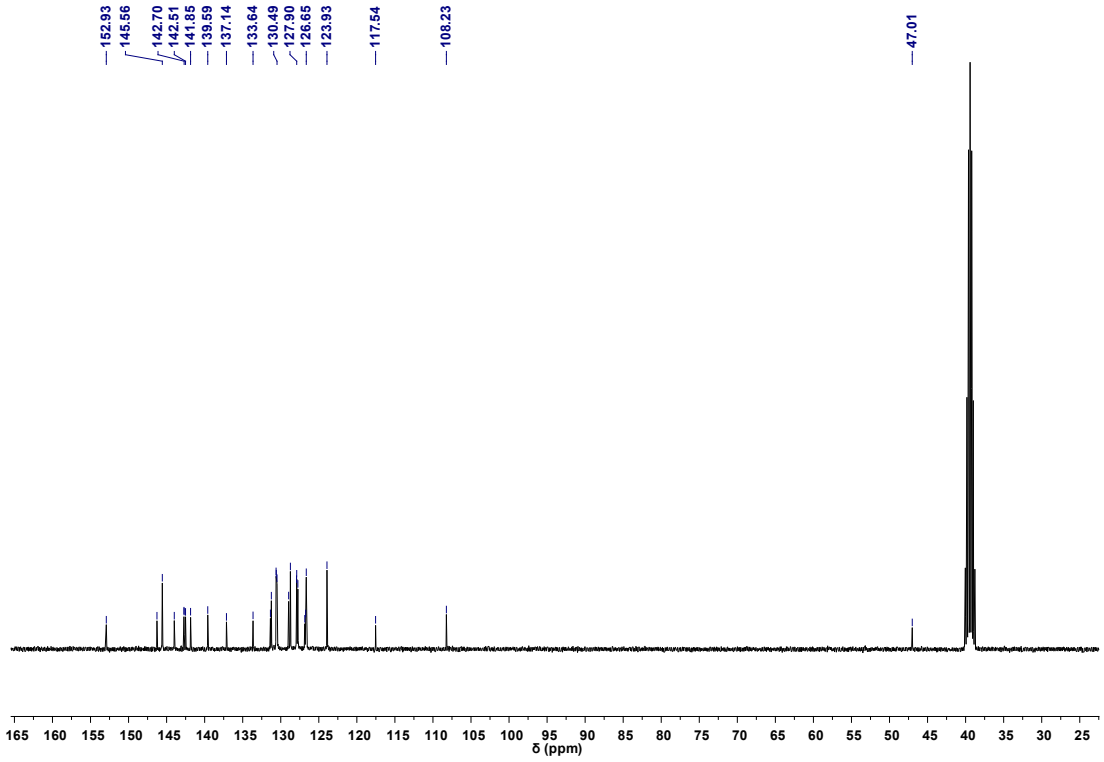

Fig. S27 ^{13}C NMR spectrum of TCPyP **(**in DMSO-d_6**)**.

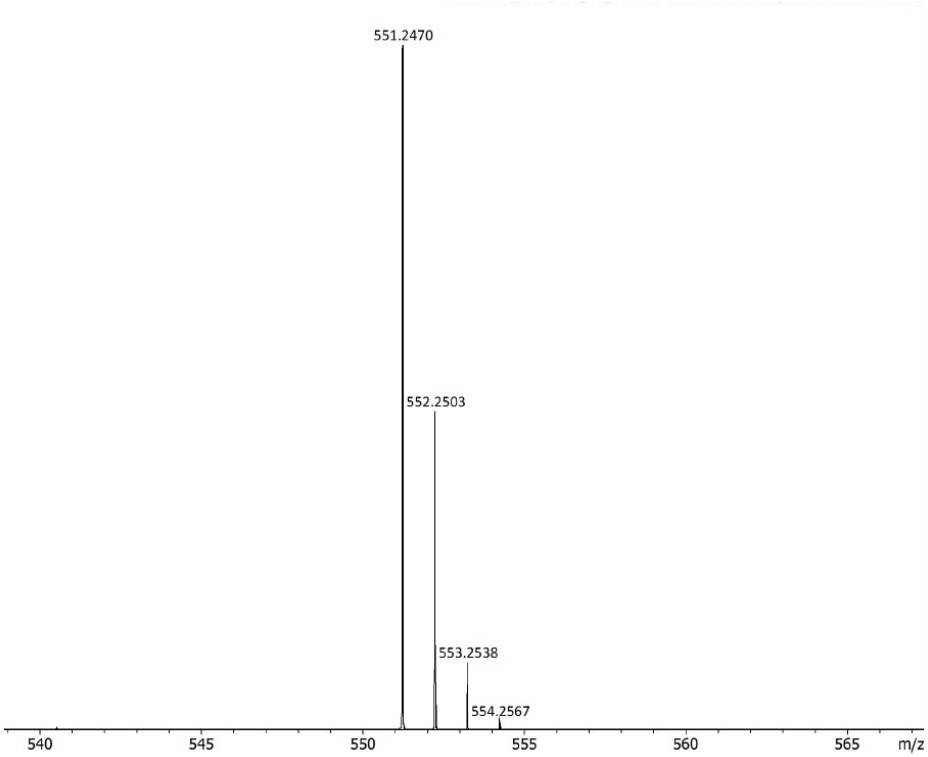

Fig. S28 ESI-MS of TCPyP.

Table S3. Crystal data and structure refinement for the three single crystals

Compound	TCPy	TCPyP
formula	$C_{40}H_{28}N_2$	$C_{41}H_{31}F_6N_2P$
fw	536.64	696.65
crystal system,	monoclinic	monoclinic
T / K	150.00(10)	150.00(10)
space group	P 1 21/c 1	P 1 21/c 1
a/Å	28.245(3)	31.7616(9)
b /Å	5.6181(4)	9.2797(2)
c/Å	18.2359(14)	12.6007(4)
α/ °	90	90
β/ °	100.631(8)	96.471(3)
γ/ °	90	90
V/Å^3, Z	2844.0(4), 4	3690.24(18), 4
F (000)	1128	1440
crystal size / mm^3	0.22×0.15×0.12	0.15×0.08×0.07
reflections collected / unique	8473/5571	12818/7240
(R_{int})	(R_{int} = 0.0371)	(R_{int} = 0.0249)
obsd reflns [I≥2σ(I)]	4407	6250
data/restraints/parameter	5571/0/379	7240/0/452
D_c/ Mg·m^{-3}	1.253	1.254
μ/ mm^{-1}	0.557	1.184
goodness-of-fit on F^2	1.085	1.050
R_1, [a] wR_2 [b] [I≥2σ(I)]	0.1115, 0.2983	0.0790, 0.2157
R_1, wR_2 (all data)	0.0537, 0.1280	0.0861, 0.2223

[a] $R_1 = \Sigma \mid |F_o| - |F_c| \mid / \Sigma |F_o|$. [b] $wR_2 = [\Sigma[w(F_o^2 - F_c^2)^2]/\Sigma w(F_o^2)^2]^{1/2}$, where $w = 1/[^2(F_o)^2 + (aP)^2 + bP]$ and $P = (F_o^2 + 2F_c^2)/3$

References

1. B. Xu, W. Li, J. He, S. Wu, Q. Zhu, Z. Yang, Y.-C. Wu, Y. Zhang, C. Jin, P.-Y. Lu, Z. Chi, S. Liu, J. Xu and M. R. Bryce, *Chem. Sci.*, 2016, **7**, 5307-5312.
2. E. R. Johnson, S. Keinan, P. Mori-Sanchez, J. Contreras-Garcia, A. J. Cohen and W. Yang, *J. Am. Chem. Soc.*, 2010, **132**, 6498.
3. T. Lu and F. Chen, *J. Comput. Chem.*, 2012, **33**, 580.
4. C. Lefebvre, G. Rubez, H. Khartabil, J. C. Boisson, J. Contreras-Garcia and E. Henon, *Phys. Chem. Chem. Phys.*, 2017, **19**, 17928.
5. W. Hu, L. Guo, L. Bai, X. Miao, Y. Ni, Q. Wang, H. Zhao, M. Xie, L. Li, X. Lu, W. Huang and Q. Fan, *Adv. Healthc. Mater.*, 2018, **7**, e1800299.
6. H. Chen, Y. Tang, H. Shang, X. Kong, R. Guo and W. Lin, *J. Mater. Chem. B*, 2017, **5**, 2436.
7. Nikolay S. Makarov, Mikhail Drobizhev and A. Rebane, *Opt. Express*, 2018, **16**, 4029.